



# Biosorption of malachite green dye over *Spirulina platensis* mass: process modeling, factors optimization, kinetic, and isotherm studies

Ziaeddin Bonyadi<sup>1,2</sup> · Elaheh Nasoudari<sup>1,2</sup> · Maryam Ameri<sup>3</sup> · Vahid Ghavami<sup>2,4</sup> · Mahmoud Shams<sup>1,2</sup> · Mika Sillanpää<sup>5,6</sup>

Received: 22 November 2021 / Accepted: 25 April 2022 / Published online: 20 May 2022  
© The Author(s) 2022

## Abstract

*Spirulina platensis* is one of the types of blue-green algae that was used as a biosorbent in this study. The aim of this study was to investigate the efficiency of *S. platensis* in removing MG from aqueous solutions and also to evaluate the biosorbent capacity using different kinetic models and isotherms. To obtain the optimum condition for MG biosorption using BBD, input factors included the initial level of MG 20–200 mg.L<sup>-1</sup>, dose of *S. platensis* (0.1–1.5 g.L<sup>-1</sup>), pH (4–9), and contact time (5–80 min). The statistical method of BBD was considered to evaluate the removal rate of MG dye from aqueous solutions. The prediction of MG removal efficiencies and the evaluation of variable interactions were performed using a polynomial equation. The maximum removal efficiency of MG was obtained as 94.12% under MG level of 100.54 mg.L<sup>-1</sup>, pH of 7.57, contact time of 52.43 min, and *S. platensis* dose of 0.98 g.L<sup>-1</sup>. The removal MG efficiency enhanced with the increase in pH, reaction time, and *S. platensis* dose, and reduced with the decrease in MG level. The quadratic model suggested that the pH had a high impact on MG removal. The isotherms and kinetics data could be properly illustrated by the Freundlich model and the pseudo-second-order equation. Thermodynamic factors, including  $\Delta G^0$ ,  $\Delta H^0$ , and  $\Delta S^0$  showed the adsorption of MG onto *S. platensis* was spontaneous and exothermic. The acquired findings also showed that the physisorption mechanism mainly govern the MG sorption process. As a result, *S. platensis* showed excellent adsorptive properties and hence could be offered as a viable option for eliminating MG from aqueous solutions.

**Keywords** Malachite green · *Spirulina platensis* · Box–Behnken design · Optimization · Biosorption

## Abbreviations

MG	Malachite green	$\Delta S^0$	Standard entropy
$\Delta G^0$	Standard Gibbs free energy	SEM	Scanning electron microscope
$\Delta H^0$	Standard enthalpy	FT-IR	Fourier-transform infrared spectroscopy

✉ Ziaeddin Bonyadi  
Bonyadz@mums.ac.ir

✉ Mika Sillanpää  
mikaesillanpaa@gmail.com  
Elaheh Nasoudari  
Elahe\_nasoudari@yahoo.com

Maryam Ameri  
Ma.ameri65@gmail.com

Vahid Ghavami  
Ghavamiv@mums.ac.ir

Mahmoud Shams  
Shamsmh@mums.ac.ir

<sup>2</sup> Social Determinants of Health Research Center, Mashhad University of Medical Sciences, Mashhad, Iran

<sup>3</sup> Industrial Microbial Biotechnology Department, Academic Center for Education, Culture and Research, Research Institute for Industrial Biotechnology, Mashhad, Iran

<sup>4</sup> Department of Biostatistics and Epidemiology, School of Health, Mashhad University of Medical Sciences, Mashhad, Iran

<sup>5</sup> Faculty of Science and Technology, School of Applied Physics, University Kebangsaan Malaysia, 43600 Bangi, Selangor, Malaysia

<sup>6</sup> International Research Centre of Nanotechnology for Himalayan Sustainability (IRCNSH), Shoolini University, Himachal Pradesh, Solan 173212, India

<sup>1</sup> Department of Environmental Health Engineering, School of Health, Mashhad University of Medical Sciences, Mashhad, Iran

BBD Box–Behnken design  
 $Q_e$  Biosorbent capacity

## Introduction

Synthetic dyes are extensively applied in a variety of industries and laboratories to colorize the products and for analytical purposes. A huge volume of colored wastewaters especially from the industrial sector is responsible for adverse environmental consequences (Dehghani et al. 2017). In the case of the textile industry alone, reports show a discharge of approximately 100 tons of dyes into water bodies each year. The discharge of industrial dyes to rivers and lakes even at low levels can increase the amount of turbidity (Mazloomi et al. 2018; Ramavandi et al. 2019).

Until now, different treatment methods such as electrocoagulation and chemical precipitation, oxidation, adsorption, ion exchange and biological methods were applied for dye laden wastewaters (Adel et al. 2021; Ameri et al. 2020; Signorelli et al. 2021; Sinha et al. 2021). Among these, adsorption technique is identified as a versatile and promising technique due to its advantages like appropriateness for removal of the low level of contaminants, the potential for adsorbent reuse, and easiness of design and operation (Davodi et al. 2019; Dehghani et al. 2020). Recently, different adsorbents, including amphiphilic graphene aerogel (Tang et al. 2019), activated carbon derived from the peel of pomegranate fruit (Ahmad et al. 2020), algal activated carbon/Fe<sub>3</sub>O<sub>4</sub> magnetic composite (Foroutan et al. 2019), and biochars from marine *Chlorella sp.* (Amin et al. 2020) were used for the removal of azo dyes from aqueous environments.

Biosorption, a unique form of adsorption that involves dead or alive biological materials, has been gaining researchers' interest. Biosorption brings a wide range of advantages such as independency to chemicals, environmentally benignness, global availability, economic benefits, effectiveness, and avoidance of sludge processing problems (Aliasghar Navaei et al. 2019; Sadeghi et al. 2019). Algae, single-cell organisms living in water bodies, were often observed as the algal biomasses in aqueous environments (Gül et al. 2019; Nasoudari et al. 2021). Malachite green is an organic compound that is frequently applied in aquaculture to protect aquatic animals from being infected by pathogenic microorganisms (Fig. 1) (Afshin et al. 2020). Shreds of evidence show that MG could pose detrimental effects on the liver and lung of experimental animals (Huang and Chien 2019). The entrance of wastewater effluents, containing synthetic dyes, into aqueous environments is worrying. Latest researches focus on the application of algae to remove textile dyes from water containing dyes and other pollutant (Ebrahimi et al. 2016; Omar et al. 2018; Preeti and Veena, 2017; Rezaee

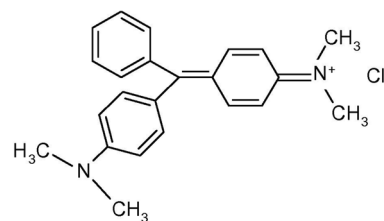


Fig. 1 Structural formula of malachite green dye

et al. 2006b). *Spirulina (Arthrospira) platensis* is a species of microalgae. *S. platensis* is easy to culture, high in nutrients and protein, and readily digestible. *S. platensis* can also promote development and improve the digestive system by stimulating the secretion and activity of some digestive enzymes (Jiang et al. 2022). Thus, the current research was conducted with the aim of optimizing MG biosorption from aqueous solutions by *S. platensis* using BBD. The mechanisms of MG biosorption on *S. platensis* were analyzed using kinetic, adsorption and thermodynamic models.

## Materials and methods

### Chemicals and reagents

The MG dye with the formula of C<sub>23</sub>H<sub>25</sub>N<sub>2</sub> was ordered from Merck Co. (Fig. 1). Specify chemical matter used were of analytical grade. The MG dye solutions in the study were obtained from a stock solution of 500 mg. L<sup>-1</sup> with distilled water.

### Biosorbent preparation

The cyanobacteria, *S. platensis* (abdf 2224), was locally purchased from the Iranian National Algae Culture Collection, Tehran, Iran. The growth of this algae was conducted using Zarrouk's Medium under constant light (3000 lx) and temperature (25 ± 1 °C). The culture was centrifuged at 4000 rpm for 10 min to remove the medium. After the separation of algal cells, those were dried at a temperature of 80 °C for 12 h. Finally, the contents were stored in a desiccator at room temperature to be used as a biosorbent.

### Characteristic measurements

The characterization of *S. platensis* was carried out by methods such as SEM and FT-IR. The FT-IR spectrometer (Broker victor 22) was used for determining the functional groups in the *S. platensis* surface and the interaction between the existing functional groups and MG after the biosorption process.

### Batch biosorption experiments

To figure out the effect of biosorption conditions on MG removal, the impact of different parameters including the initial level of dye (20–200 mg. L<sup>-1</sup>), pH (4–9), contact time (5–80 min), and biosorbent dose (0.1–1.5 g. L<sup>-1</sup>) were studied (Table 1).

The factors and their studied ranges were determined according to the literature review (Gül et al. 2019). The dye solutions were agitated in a reaction vessel under a constant speed of 300 rpm. Except for those mentioned, the experiments were conducted at room temperature. Furthermore, all biosorption experiments were conducted in duplicate. After the biosorption occurred, the solutions centrifuged and the remaining MG dye was measured in the supernatant by the spectrophotometric technique at λ<sub>max</sub> of 618 nm. The removal efficiency and q<sub>e</sub> were being considered as responses for analysis of the data. The removal efficiency of MG was measured using the following formula:

$$\text{Removal efficiency}\% = \frac{(C_0 - C_e) \times 100}{C_0} \tag{1}$$

where C<sub>0</sub> is the MG concentration in the control sample (mg. L<sup>-1</sup>) and C is the MG concentration in the treated solution after a given time (mg.L<sup>-1</sup>).

The amount of MG adsorbed per unit biosorption was calculated using the following formula:

$$q_e = \frac{(C_0 - C_e) \times V}{W} \tag{2}$$

where V and W are dye solution volume (mL), and *S. platensis* biomass mass (g), respectively (Davodi et al. 2019).

Furthermore, the biosorbent reusability was assessed through consecutive biosorption-desorption cycles using the same biomass. Desorption cycles were conducted under acidic conditions in contact with the loaded biosorbent in a shaker for 1 h, at 250 rpm, and 28 °C. After desorption, the biosorbent was centrifuged at 2000 g and thoroughly washed with water before another biosorption cycle.

**Table 1** Range and levels of independent factors used for the MG biosorption

Factor	Factor level			
	Code	-1	0	+1
Contact time (min)	A	5	42.5	80
MG (mg. L <sup>-1</sup> )	B	20	110	200
pH	C	4.0	6.5	9.0
<i>S. platensis</i> dosage (g. L <sup>-1</sup> )	D	0.1	0.8	1.5

### Study matrix

As mentioned earlier, a statistical method was adopted for the entire design, modeling, and optimization of dye removal study. BBD was considered to set a model to maximize the biosorption of MG onto *S. platensis*. The BBD approach is a superior alternative to its traditional "one factor at a time" counterpart because it determines the optimal condition and interaction effects of variables. BBD is a three-level rotatable or nearly rotatable quadratic design in which the variables studied at their midpoints (± 1) and the center point (0)(Wan et al. 2018). Table 1 shows the ranges and values of studied factors. In this work, 29 experimental runs, based on the BBD design, were conducted to study the four process factors. The data obtained in the experiments were analyzed using a second-order polynomial model to find the linear and quadratic effects of factors on MG removal. The ANOVA analysis uses the following equation (Eq. 3) to describe the process

$$Y = \beta_0 + \sum_{i=1}^k \beta_i X_i + \sum_{i=1}^k \beta_{ii} X_i^2 + \sum_{i=1}^{k-1} 1 \sum_{j=1}^k \beta_{ij} X_i X_j + \epsilon \tag{3}$$

In the Eq. 3, Y is the response (MG removal), X<sub>i</sub> and X<sub>j</sub> are coded factors, β<sub>0</sub> is a constant level, β<sub>i</sub>, β<sub>ii</sub>, and β<sub>ij</sub> are the first-order effects, second-order effects, and interaction impacts regression coefficients and ε is the random error (Balasubramani et al. 2020).

After optimization isotherm and kinetic studies were conducted. To obtain equilibrium data to fit the most known isotherm models, including Freundlich, Langmuir, Temkin, and Dubinin–Radushkevich, the series of batch experiments were performed in the presence of several MG levels (10 to 150 mg. L<sup>-1</sup>). The pH of the solution was adjusted to 7.49 as obtained in optimization. Kinetic studies also composed a necessary section of the sorption survey that reveals important data for real treatment system design. Kinetic experiments were carried out in the presence of fixed 1.06 mg. L<sup>-1</sup> adsorbent mass. At various time stages (10, 20, 30, 40, and 50 min), samples taken from solutions contained dye level, ranging from 10–150 mg. L<sup>-1</sup>. Finally, the kinetic information fitted to pseudo-first-order, pseudo-second-order, and intra-particle diffusion models.

## Results and discussion

### Characterization of *S. platensis*

#### FTIR

Determination of MG biosorption behavior was conducted by FTIR analysis. Figure 2 shows FTIR spectra of fresh and used *S. platensis*. The FTIR spectrum of *S. platensis* before

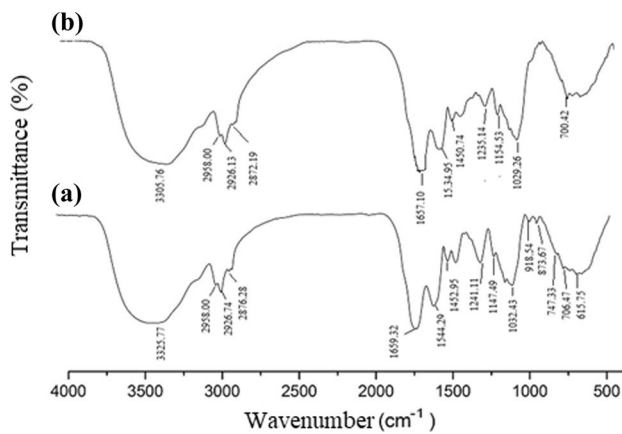


**Fig. 2** FTIR Spectra of **A** Before and **B** After dye biosorption

the biosorption process displays several major intense bands, around 3325, 2958, 2926, 2876, 1659, 1544, 1452, 1241, 1147, 1032, 918, 873, 747, 706, and 615  $\text{cm}^{-1}$  (Fig. 2A). The peak at 3325  $\text{cm}^{-1}$  was related to the O–H bond stretching mixed with the  $\text{NH}_2$  group. The absorption peaks at 2958, 2926, and 2876  $\text{cm}^{-1}$  may be caused by the stretching vibrations of  $\text{CH}_3$  and  $\text{CH}_2$  groups. In Fig. 2B, after MG biosorption, the situation of some peaks has shifted. The alteration of the 3325  $\text{cm}^{-1}$  peak to 3305  $\text{cm}^{-1}$  offers the attachment of MG dye on –OH and –NH group (Kousha et al. 2013). The shift in a peak at 1659.32 to 1657.10  $\text{cm}^{-1}$  signifies the involvement of the C=O group. Also, the peak at 1032.43  $\text{cm}^{-1}$  was shifted to 1029.26  $\text{cm}^{-1}$ , which signifies the involvement of a carboxylate group ( $\text{COO}^-$ ) in the adsorption of basic MG dye.

## SEM

Figure 3 indicates the SEM of the raw *S. platensis*. The SEM analysis showed that the surface of *S. platensis* had

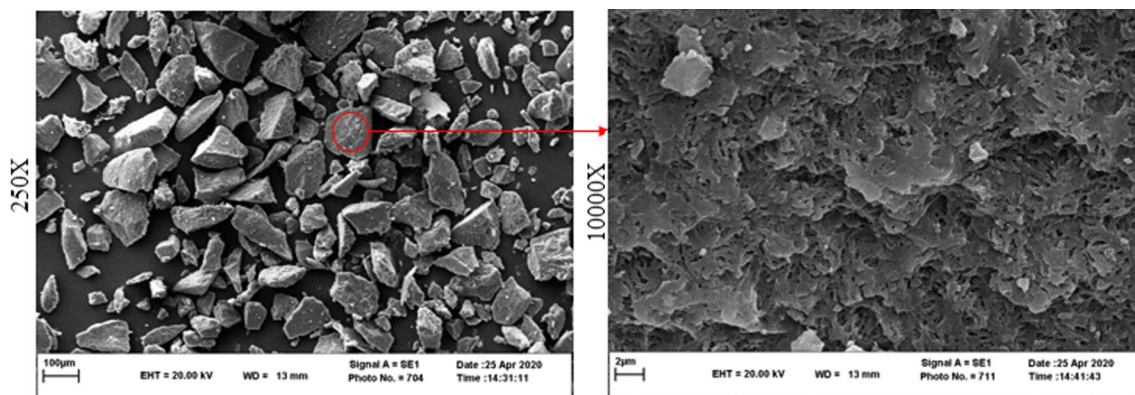


**Fig. 3** SEM image of the raw *S. platensis*

nonhomogeneous with irregular and rough surfaces with different pores. With regard to the structural form *S. platensis*, it can be said that this algae has a large and accessible surface area for the biosorption of dye.

The curve of initial pH versus final pH of *S. platensis* in suspension is indicated in Fig. 4. This figure shows that zero-point charge ( $\text{pH}_{\text{zpc}}$ ) of the studied algae is 6.75. When the suspension pH is lower than 6.75, the charge on the algal cell wall becomes positive and at the solution pH values higher than 6.75 the *S. platensis* surface is negatively charged. The  $\text{pH}_{\text{zpc}}$  parameter is one of the suitable methods for understanding the biosorption mechanisms (Dotto et al. 2012).

## Modeling of the MG removal efficiency

The design matrix employed for MG removal by *S. platensis* biomass and the experimental responses obtained is given in Table 2. The optimized levels for MG concentration, *S. platensis* dose, pH, and contact time were obtained to be 80.97  $\text{mg.L}^{-1}$ , 0.7  $\text{g.L}^{-1}$ , 8.89 and 42.52 min, respectively. At these conditions, the predicted MG removal percentage was more than 87% with desirability 1. Conduction of similar experiments at specified optimum conditions reveal the

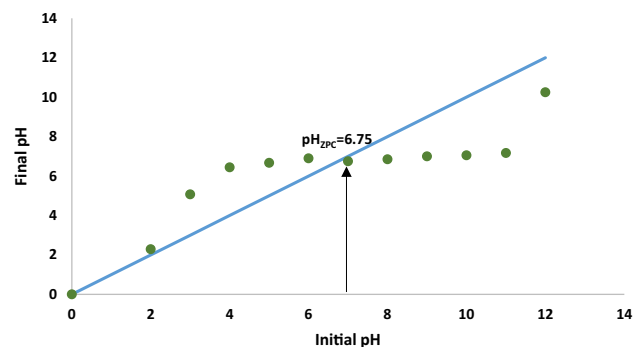


**Fig. 4** Effect of pH on zeta potential of the *S. platensis*

**Table 2** BBD matrix for MG removal by *S. platensis*

Run no	Coded variable				Removal (%)	Run no	Coded variable				Removal (%)
	A	B	C	D			A	B	C	D	
1	-1	0	0	1	74.2	16	1	0	1	0	80.6
2	-1	0	1	0	78.2	17	1	0	-1	0	52
3	1	-1	0	0	69.5	18	0	-1	1	0	71
4	0	0	1	1	85.5	19	0	-1	0	1	64.6
5	-1	1	0	0	59.2	20	0	0	0	0	85.6
6	-1	-1	0	0	45.2	21	0	1	1	0	58.2
7	0	-1	-1	0	35.6	22	0	0	-1	-1	46
8	0	0	0	0	90.2	23	0	1	0	1	57.9
9	1	0	0	-1	74.2	24	0	0	0	0	93
10	0	-1	0	-1	65.3	25	-1	0	-1	0	45.2
11	0	0	0	0	95.5	26	0	0	0	0	84.9
12	1	0	0	1	83.1	27	0	0	-1	1	65.2
13	1	1	0	0	62.2	28	0	1	0	-1	42
14	0	0	1	-1	75.2	29	0	1	-1	0	32.2
15	-1	0	0	-1	65.1		1	0	1	0	80.6

high repeat ability of method for prediction of real removal percentage with relative deviation less than 2%.

As shown, the upper and lower range of MG removal varied from 35.6 to 95.5%, respectively. Design-Expert® Software confirmed the normality of experimental data, which is essential for ANOVA (Table 3).

A quadratic polynomial prediction formula (based on model comparison as shown in Table 4) was developed to elucidate the relationship between the MG removal and independent variables:

$$\begin{aligned}
 \text{MGremoval} = & 89.84 + 4.54A - 3.29B + 14.38C + 5.23D - 5.33 AB \\
 & - 1.10 AC - 0.05 AD - 2.35 BC + 4.15 BD - 2.23 CD - 8.31A^2 - 24.03B^2 - 16.28C^2 - 7.11 D^2
 \end{aligned}
 \tag{4}$$

This prediction model reflects how independent variables and interactions between them affect the process. The positive and negative sign before each model term shows the removal increase or inversely decreased at higher term values, respectively. Moreover, the higher the coefficient of each term is indicating the greater the level of impact on dye biosorption. Based on Eq. 4, the code of C recognized the major variable that plays the most important role in MG removal.

The adequacy of the model is illustrated in Fig. 5, where there is a good agreement between experimental MG removals with corresponding predicted values. Based on the results depicted in Fig. 5, the predicted removal is close to their obtained in the experiments which revealed the preciseness of the proposed model. However, model efficacy should be established statistically. ANOVA is available for this purpose. The results of the analysis of variance for a 95% confidence interval are given in Table 5. As shown, the F-value for the model is 21.25,

which indicated that the model is significant. The p-value for lack of fit (LOF) test is 0.39, which reveals the fitness of the prediction model. Moreover, the regression has a good R<sup>2</sup>, which is close to 1 and in the range of ±0.2 to the adjusted correlation coefficient (R<sup>2</sup><sub>adj</sub> = 0.91).

All mentioned statistical parameters confirmed the adequacy of the developed model for MG removal prediction. For each model term in Table 5, the p-value < 0.001 means that its effect on MG removal is statically

**Table 3** Statistical adequacy evaluation of models

Source	Sequential <i>p</i> value	Lack of fit <i>p</i> value	Adjusted R <sup>2</sup>	Predicted R <sup>2</sup>
Linear	0.0196	0.0127	0.2707	0.1802
2FI	0.9898	0.0073	0.0696	-0.2598
Quadratic	<0.0001	0.3972	0.9101	0.7829
Cubic	0.2641	0.5288	0.9361	0.4469



**Table 4** Coefficients estimation for the quadratic model of MG removal by *S. platensis*

Factor	Coefficient Estimate	df	Standard Error	95% CI Low	95% CI High	VIF
Intercept	89.84	1	2.34	84.83	94.85	
A-Time	4.54	1	1.51	1.31	7.77	1
B-Conc	- 3.29	1	1.51	- 6.52	- 0.06	1
C-pH	14.37	1	1.51	11.14	17.61	1
D-Dose	5.23	1	1.51	1.99	8.46	1
AB	- 5.32	1	2.61	- 10.92	0.27	1
AC	- 1.10	1	2.61	- 6.70	4.50	1
AD	- 0.0500	1	2.61	- 5.65	5.55	1
BC	- 2.35	1	2.61	- 7.95	3.25	1
BD	4.15	1	2.61	- 1.45	9.75	1
CD	- 2.23	1	2.61	- 7.82	3.37	1
A <sup>2</sup>	- 8.31	1	2.05	- 12.70	- 3.91	1.08
B <sup>2</sup>	- 24.03	1	2.05	- 28.43	- 19.64	1.08
C <sup>2</sup>	- 16.28	1	2.05	- 20.68	- 11.89	1.08
D <sup>2</sup>	- 7.11	1	2.34	84.83	94.85	1.08

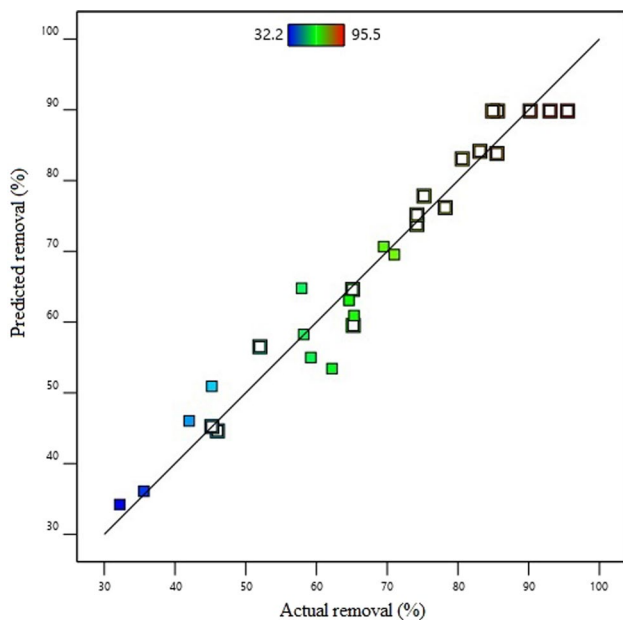


**Fig. 5** Distribution of experimental vs. predicted removal for MG adsorption onto *S. platensis*

significant. As shown, for the present work all individual variables and some first and second-order terms show significant effects on the response. Conduction of similar experiments at specified optimum conditions reveals the high repeatability of the procedure for prediction of actual removal rate with relative deviation less than 2%.

**Main and interaction effects**

The influence of studied variables is graphed by response surface plots in Fig. 6. The 3D plots clearly illustrate the

**Table 5** Analysis of variance for the quadratic model of MG removal by *S. platensis*

Source	Sum of Squares	df	Mean Square	F-value	p value
Model	8112.85	14	579.49	21.25	<0.0001
A- Time	247.52	1	247.52	9.08	0.0093
B- Conc	130.02	1	130.02	4.77	0.0465
C- pH	2479.69	1	2479.69	90.94	<0.0001
D- Dose	327.61	1	327.61	12.01	0.0038
AB	113.42	1	113.42	4.16	0.0607
AC	4.84	1	4.84	0.1775	0.6799
AD	0.0100	1	0.0100	0.0004	0.9850
BC	22.09	1	22.09	0.8101	0.3833
BD	68.89	1	68.89	2.53	0.1343
CD	19.80	1	19.80	0.7262	0.4084
A <sup>2</sup>	447.66	1	447.66	16.42	0.0012
B <sup>2</sup>	3746.34	1	3746.34	137.40	<0.0001
C <sup>2</sup>	1719.70	1	1719.70	63.07	<0.0001
D <sup>2</sup>	327.67	1	327.67	12.02	0.0038
Residual	381.74	14	27.27		
Lack of Fit	297.20	10	29.72	1.41	0.3972
Pure Error	84.53	4	21.13		
Cor Total	8494.59	28			
R <sup>2</sup>	0.9551		Predicted R <sup>2</sup>	0.7829	
Adjusted R <sup>2</sup>	0.9101		Adeq. Precision	14.8135	

possible interaction between studied variables. As shown in Fig. 6a, the increase in *S. platensis* biomass dose was favorable for the MG removal efficacy. This is a normal behavior of most sorption processes. Based on the biosorption theory,

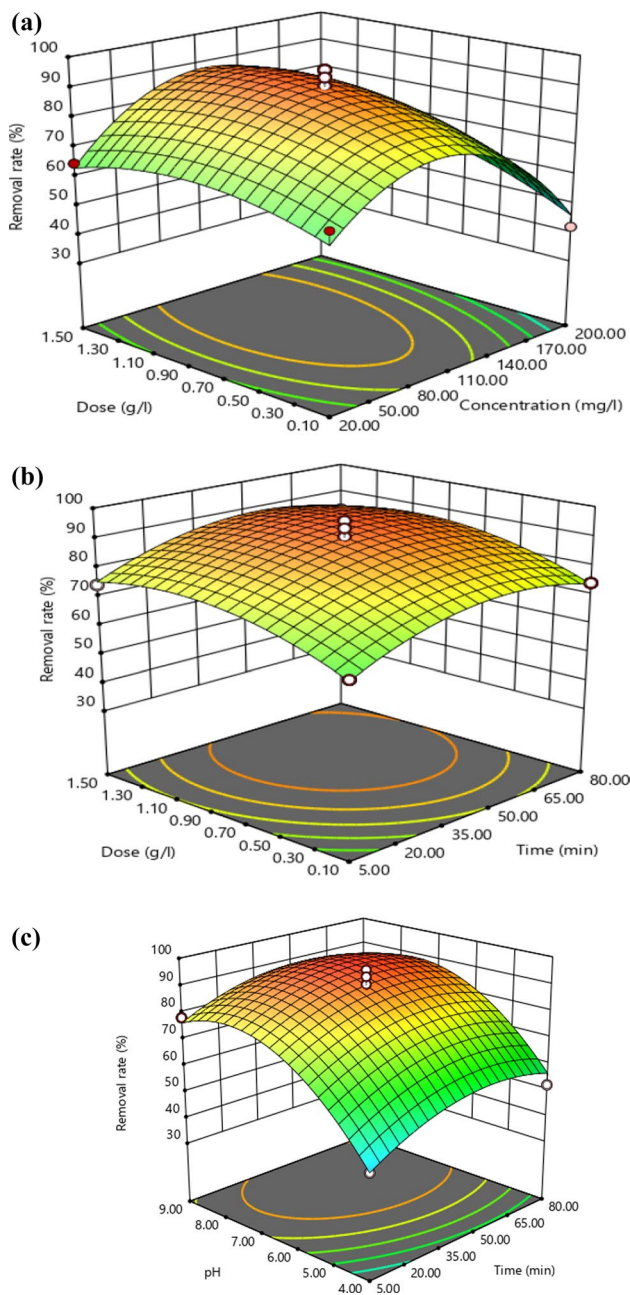


**Fig. 6** Response surface plot about the effects of **a** pH vs. time, **b** *S. platensis* vs. time and **c** *S. platensis* vs. MG

the contaminants are attracted to the sorption sites on the biosorbent surface (Kousha et al. 2013). The availability of sorption sites is directly related to the mass of biosorbent added to the solution. At lower MG levels, the adsorption rate is higher due to the existence of more energetically active sites on the biosorbent surface. The reason for the sharp decline of removal rate with the enhance in the initial MG level is the lack of sufficient surface area to accommodate more dye molecules available in the solution (Ramavandi et al. 2019). From the results of Fig. 6b,

the contact time shows an incremental effect on biosorption efficiency. This behavior could attribute to the fact that the sorption process occurs gradually and the MG molecules need time to be adsorbed on sorption sites. About the saturation of the biosorbent site on the outer interface of the biosorbent, a decrease in dye removal happened when mixing continued beyond the optimum time value (Mohebbad et al. 2019; Rangabhashiyam et al. 2018). The solution pH is another critical factor that can affect the biosorption performance of *S. platensis*. This factor influences the surface charge of biosorbent and ionization state of MG molecules (Fig. 6c). Under the alkaline situation, the MG dissociated to give a negative charge to dye molecules. On the other hand, the isoelectric point ( $\text{pH}_{\text{PZC}}$ ) of *S. platensis* biomass was determined to be 6.68. It means the *S. platensis* surface has a net positive charge at pH smaller than 6.68. Therefore, the increase of MG biosorption at low pH could be attributed to the electrostatic attraction between MG molecules and *S. platensis* cell surface (Rezaee et al. 2006a). Whereas, at a pH above  $\text{pH}_{\text{PZC}}$ , due to the deprotonation of functional groups, a negative net charge will be generated on the cell surface, which leads to weak electrostatic attraction between the biosorbent and dye molecules (Al-Ghouti and Da'ana, 2020). After all adsorption sites are saturated, the biosorption rate slows down and equilibrium is gradually reached. Similar study was carried out for MG biosorption by *Pithophora sp.* at pH 5.0 (varied in the range 2–7), algae dose of 0.03 g/30 mL, temperature 30 °C, and initial dye level up to 100  $\text{mg}\cdot\text{L}^{-1}$  within 5 h (Kumar et al. 2005). In the study of Sun et al. from China, biosorption of MG was carried out in the range of 2 to 11 which reached equilibrium at 60 min for 50  $\text{mg}\cdot\text{L}^{-1}$  dye level (Sun et al. 2008).

### Isotherm and kinetic models

The adsorption isotherm is a crucial part of a sorbate-sorbent study that describes the interaction mechanisms between the biosorbent and the adsorbate at stable temperature (Al-Ghouti and Da'ana, 2020). The sorption models also broaden our understanding of the economy of the sorption system. In collecting the experimental equilibrium data, the factors are set at their optimal values as obtained as pH 7.49, contact time of 49 min, dye level of 130.55  $\text{mg}\cdot\text{L}^{-1}$  and *S. platensis* dose of 1.06  $\text{mg}\cdot\text{L}^{-1}$  (Table 6). To address the biosorption isotherm, the experimental equilibrium information were studied using Langmuir, Freundlich, Temkin, and Dubinin–Radushkevich models. The kinetic and isotherm parameter factors fitted for MG removal by *S. platensis* were listed in Table 6. As shown, the equilibrium data has a good agreement with the Freundlich model. A higher determination coefficient for the Freundlich model describes multilayer adsorption and heterogeneous sorption sites on *S. platensis* cell surface (Veloso et al. 2020). The same results

**Table 6** The kinetic and isotherm parameters fitted for MG removal by *S. platensis*

Kinetic Model	Linear Form	Parameter	Value			
			10 mg.L <sup>-1</sup>	50 mg.L <sup>-1</sup>	100 mg.L <sup>-1</sup>	150 mg.L <sup>-1</sup>
Pseudo- first order	$\text{Log}(q_e - q_t) = \log q_e - \frac{k_1}{2.303} \cdot t$	$q_{e,\text{cal}}$ (mg.g <sup>-1</sup> )	0.99	0.99	0.91	0.98
		$K_1$ (min <sup>-1</sup> )	- 1.10	0.15	1.34	2.68
		$R^2$	0.99	0.99	0.99	0.98
Pseudo- second order	$\frac{t}{q_t} = \frac{1}{k_2 q_e} + \frac{1}{q_e} \cdot t$	$q_{e,\text{cal}}$ (mg.g <sup>-1</sup> )	3.24	15.33	30.30	39.52
		$K_2$ (min <sup>-1</sup> )	0.22	0.05	0.05	0.02
		$R^2$	0.99	0.99	0.99	0.99
Intra-particle diffusion	$qt = k_p \cdot t^{0.5} + c$	$K_p$ (mg.g <sup>-1</sup> .min <sup>-0.5</sup> )	0.086	0.04	0.50	0.81
		$R^2$	0.53	0.70	0.98	0.85
Isotherm model	Linear form	Parameter	Value			
Langmuir	$\frac{C_e}{q_e} = \frac{1}{q_m} C_e + \frac{1}{q_m b}$	$q_{\text{max}}$ (mg.g <sup>-1</sup> )	103.09			
		$K_L$ (L.mg <sup>-1</sup> )	0.015			
		$R^2$	0.82			
Freundlich	$\text{Log } q_e = \log K_F + \frac{1}{n} \log C_e$	$K_F \text{mg.g}^{-1} (\text{L.mg}^{-1})^{1/n}$	2.11			
		$N$	1.26			
		$R^2$	0.99			
Temkin	$q_e = B_1 \ln k_t + B_1 \ln C_e$	$k_t$ (L.mg <sup>-1</sup> )	13			
		$B_1$	12.19			
		$R^2$	0.84			
Dubinin–Radushkevich	$\ln q_e = \ln q_m - \beta \epsilon^2$	$q_{\text{max}}$ (mg.g <sup>-1</sup> )	25.68			
		$\beta$	$1.67 \times 10^{-6}$			
		$R^2$	0.88			

are reported about MG biosorption by like *Pithophora sp.* (Kumar et al. 2006) and green algae (Al-Homaidan et al. 2018). Also, the highest maximum adsorption capacity of *S. platensis* was acquired to be 103.09 mg.g<sup>-1</sup> according to the Langmuir model. Table 3 demonstrates a comparison between the biosorption capacities of MG dye with earlier studies.

Adsorption kinetic also provides necessary information in modeling and designing the process. Determining the adsorption mechanism and its rate-limiting steps also are achievable by kinetic study (Mohammed and Kareem, 2019). The experimental kinetic data were fitted in

pseudo-first-order, pseudo-second-order, and intra-particle diffusion models. The results of kinetic modeling and their coefficients were shown in Table 6. As shown, the pseudo-second-order model has a higher  $R^2$  value compared to other models. Moreover, the calculated  $Q_e$  or equilibrium adsorption capacity for the pseudo-second-order model is close to its correspondence experimental level (Table 7).

### Sorption thermodynamic

Table 8 displays thermodynamics parameters for malachite green sorption onto *S. platensis*. The  $\Delta G^\circ$  value for MG

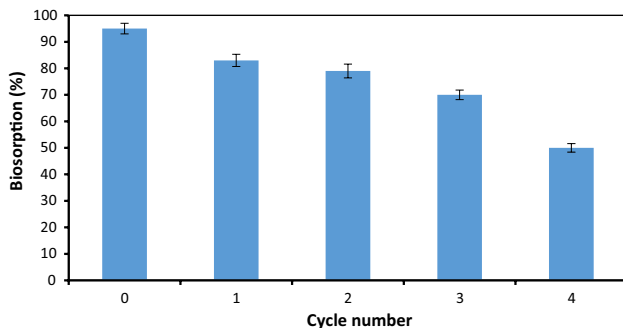
**Table 7** Comparison of Langmuir biosorption capacities of MG with results from previous studies

Biosorbent	Adsorbate MG (mg.g <sup>-1</sup> )	Reference
<i>Carica papaya</i> wood	52.63	Rangabhashiyam et al. (2018)
Tamarind fruit shell	1.95	Saha et al. (2010)
Rubber wood sawdust	36.50	Kumar and Sivanesan (2007)
<i>Caulerpa racemosa</i> var. <i>cylindracea</i>	25.67	Bekçi et al. (2009)
<i>Annona squamosa</i> seed	25.91	Santhi et al. (2016)
Banana pseudo-stem fiber	26.50	Neha et al. (2011)
<i>Spirulina platensis</i>	103.09	Current study



**Table 8** Thermodynamics parameters for malachite green sorption onto *S. platensis*

T (K)	$\Delta G^\circ$ (kJ.mol <sup>-1</sup> )	$\Delta H^\circ$ (kJ.mol <sup>-1</sup> )	$\Delta S^\circ$ (J (mol.K) <sup>-1</sup> )
298.15	- 4.29	- 39.01	- 0.11
308.15	- 2.39		
318.15	- 2.09		

**Fig. 7** Effect of reusability of the biosorbent on removal efficiency

sorption at various temperatures has been varied between  $- 2.09$  kJ.mol<sup>-1</sup> and  $- 4.29$  kJ.mol<sup>-1</sup>. So,  $\Delta G^\circ$  values obtained are below 20 kJ.mol<sup>-1</sup>, showing that the method follows the physisorption mechanism (Ahmad et al. 2014). Also, the negative  $\Delta G$  value showed the favorable and spontaneous nature of the biosorption process. The  $\Delta H^\circ$  value at the temperature in the range of 298.15 K to 328.15 K is obtained  $- 39.01$  kJ.mol<sup>-1</sup>. This value is lower than 40 kJ.mol<sup>-1</sup>; which further supports the fact that the adsorption process follows the physical mechanism. The  $\Delta S^\circ$  value at the temperature in the range of 298.15 K to 318.15 K was obtained  $- 0.11$  J. mol<sup>-1</sup>. The negative value of  $\Delta H^\circ$  shows that the MG sorption is exothermic and the negative value of  $\Delta S^\circ$  indicates the decline in randomness (Danish et al. 2018).

### Reusability of the *S. platensis* biomass

The major economic and environmental characteristic of a biosorbent is its reusability potential. As indicated in Fig. 7, the removal rates of MG from the first cycle up to the fourth cycle were varied from 95 to 50%, respectively. Results indicated that *S. platensis* can be used successfully at least four times after desorption for the removal of MG. Based on previous research, the biosorbents of *Carica papaya* (Adel et al. 2021) and *Sargassum swartzii* (Jerold and Sivasubramanian, 2017) preserved their adsorption capability after five and three cycles, respectively.

## Conclusion

*S. platensis* belongs to affluent blue-green microalga which is applied extensively in a variety of researches. In the present work, a green approach was opted to remove a persistent dye staff from synthetic solutions. By using a statistical methodology, the process of dye removal was modeled and optimized. The optimized levels for MG concentration, *S. platensis* dose, pH, and contact time were obtained to be 80.97 mg.L<sup>-1</sup>, 0.7 g.L<sup>-1</sup>, 8.89 and 42.52 min, respectively. According to the quadratic model, pH was found to be the major variable that plays the main role in MG removal. Moreover, based on the model, all studied variables have a positive effect on dye biosorption. The MG removal obeys the pseudo-second-order model and the Freundlich model. This describes the *S. platensis* surface to be heterogenic and multilayer adsorptive properties. Ultimately, *S. platensis* shows excellent adsorptive properties and hence could be offered as a viable option for future researches.

**Acknowledgements** Not applicable.

**Author's contributions** ZB wrote and edited the paper, and conceived and designed the experiments; EN performed the experiments and wrote the paper; MA edited the paper, MS interpretation of the data presented, VG performed the statistical analysis of the data; MS wrote and edited the paper.

**Funding** The authors would like to appreciate the financial support provided by Mashhad University of Medical Science for the MSC dissertation under Grant Number 980300.

**Data availability** All necessary data are included in the document.

## Declarations

**Conflict of interest** The authors declare that they have no conflict of interests.

**Ethical approval** This article does not contain any studies with human participants or animals performed by any of the authors.

**Open Access** This article is licensed under a Creative Commons Attribution 4.0 International License, which permits use, sharing, adaptation, distribution and reproduction in any medium or format, as long as you give appropriate credit to the original author(s) and the source, provide a link to the Creative Commons licence, and indicate if changes were made. The images or other third party material in this article are included in the article's Creative Commons licence, unless indicated otherwise in a credit line to the material. If material is not included in the article's Creative Commons licence and your intended use is not permitted by statutory regulation or exceeds the permitted use, you will need to obtain permission directly from the copyright holder. To view a copy of this licence, visit <http://creativecommons.org/licenses/by/4.0/>.

## References

- Adel M, Ahmed MA, Mohamed AA (2021) Effective removal of indigo carmine dye from wastewaters by adsorption onto mesoporous magnesium ferrite nanoparticles. *Environ Nanotechnol Monitor Manage* 65:100550
- Afshin S, Rashtbari Y, Ramavandi B, Fazlzadeh M, Vosoughi M, Mokhtari SA, Shirmardi M, Rehman R (2020) Magnetic nanocomposite of filamentous algae activated carbon for efficient elimination of cephalixin from aqueous media. *Korean J Chem Eng* 37:80–92
- Ahmad MA, Eusoff MA, Oladoye PO, Adegoke KA, Bello OS (2020) Statistical optimization of Remazol Brilliant Blue R dye adsorption onto activated carbon prepared from pomegranate fruit peel. *Chem Data Collect* 28:100426
- Ahmad MA, Puad NAA, Bello OS (2014) Kinetic, equilibrium and thermodynamic studies of synthetic dye removal using pomegranate peel activated carbon prepared by microwave-induced KOH activation. *Water Resour Ind* 6:18–35
- Al-Ghouti MA, Daana DA (2020) Guidelines for the use and interpretation of adsorption isotherm models: a review. *J Hazard Mater* 52:122383
- Al-Homaidan AA, Al-Qahtani HS, Al-Ghanayem AA, Ameen F, Ibraheem IB (2018) Potential use of green algae as a biosorbent for hexavalent chromium removal from aqueous solutions. *Saudi J Biol Sci* 25(8):1733–1738
- Aliasghar Navaei M, Alidadi H, Dankoob M, Bonyadi Z, Dehghan A, Hosseini A (2019) Biosorption of Reactive Red 120 dye from aqueous solution using *Saccharomyces cerevisiae*: RSM analysis, isotherms and kinetic studies. *Desalin Water Treat* 171:418–427
- Ameri M, Khavari-Nejad R, Soltani N, Najafi F, Bagheri A (2020) Application of immobilized microalgae for native wastewater treatment. *Int J Algae* 22(1):871
- Amin M, Chetpattananondh P, Khan MN (2020) Ultrasound assisted adsorption of reactive dye-145 by biochars from marine *Chlorella* sp. extracted solid waste pyrolyzed at various temperatures. *J Env Chem Eng* 65:104403
- Balasubramani K, Sivarajasekar N, Naushad M (2020) Effective adsorption of antidiabetic pharmaceutical (metformin) from aqueous medium using graphene oxide nanoparticles: Equilibrium and statistical modelling. *J Mol Liq* 301:112426
- Bekçi Z, Seki Y, Cavas L (2009) Removal of malachite green by using an invasive marine algae *Caulerpa racemosa* var. *cylindracea*. *J Hazard Mater* 161:1454–1460
- Danish M, Ahmad T, Majeed S, Ahmad M, Ziyang L, Pin Z, Iqbal SS (2018) Use of banana trunk waste as activated carbon in scavenging methylene blue dye: kinetic, thermodynamic, and isotherm studies. *Bioresour Technol Report* 3:127–137
- Davodi M, Alidadi H, Ramezani A, Jamali-Behnam F, Bonyadi Z (2019) Study of the removal efficiency of arsenic from aqueous solutions using *Melia azedarach* sawdust modified with FeO: isotherm and kinetic studies. *Desalin Water Treat* 137:292–299
- Dehghani MH, Dehghan A, Alidadi H, Dolatabadi M, Mehrabpour M, Converti A (2017) Removal of methylene blue dye from aqueous solutions by a new chitosan/zeolite composite from shrimp waste: Kinetic and equilibrium study. *Korean J Chem Eng* 34(6):1699–1707
- Dehghani MH, Karri RR, Yeganeh ZT, Mahvi AH, Nourmoradi H, Salari M, Zarei A, Sillanpää M (2020) Statistical modelling of endocrine disrupting compounds adsorption onto activated carbon prepared from wood using CCD-RSM and DE hybrid evolutionary optimization framework: Comparison of linear vs non-linear isotherm and kinetic parameters. *J Mol Liq* 302:112526
- Dotto G, Lima E, Pinto L (2012) Biosorption of food dyes onto *Spirulina platensis* nanoparticles: equilibrium isotherm and thermodynamic analysis. *Bioresour Technol* 103(1):123–130
- Ebrahimi A, Hashemi S, Akbarzadeh S, Ramavandi B (2016) Modification of green algae harvested from the Persian Gulf by L-cysteine for enhancing copper adsorption from wastewater: experimental data. *Chem Data Collect* 2:36–42
- Foroutan R, Mohammadi R, Razeghi J, Ramavandi B (2019) Performance of algal activated carbon/Fe<sub>3</sub>O<sub>4</sub> magnetic composite for cationic dyes removal from aqueous solutions. *Algal Res* 40:101509
- Gül Ü, Taştan B, Bayazıt G (2019) Assessment of algal biomasses having different cell structures for biosorption properties of acid red P-2BX dye. *South Afr J Botany* 127:147–152
- Huang C-Y, Chien C-H (2019) Facile Fabrication of micro/nano hierarchical SERS sensor via anisotropic etching and electrochemical treatment for malachite green detection. *App Sci* 9(23):5237
- Jerold M, Sivasubramanian V (2017) Biosorptive removal of malachite green from aqueous solution using chemically modified brown marine alga *Sargassum swartzii*. *Water Sci Technol* 75:598–608
- Jiang W, Miao L, Lin Y, Ci L, Liu B, Ge X (2022) *Spirulina (Arthrospira) platensis* as a protein source could improve growth, feed utilisation and digestion and physiological status in juvenile blunt snout bream (*Megalobrama amblycephala*). *Aquaculture Rep* 22:100932
- Kousha M, Farhadian O, Dorafshan S, Soofiani NM, Bhatnagar A (2013) Optimization of malachite green biosorption by green microalgae-*Scenedesmus quadricauda* and *Chlorella vulgaris*: application of response surface methodology. *J Taiwan Inst Chem Eng* 44(2):291–294
- Kumar KV, Ramamurthi V, Sivanesan S (2006) Biosorption of malachite green, a cationic dye onto *Pithophora* sp., a fresh water algae. *Dyes Pigm* 69:102–107
- Kumar KV, Sivanesan S (2007) Isotherms for Malachite Green onto rubber wood (*Hevea brasiliensis*) sawdust: comparison of linear and non-linear methods. *Dyes Pigm* 72(1):124–129
- Kumar KV, Sivanesan S, Ramamurthi V (2005) Adsorption of malachite green onto *Pithophora* sp., a fresh water algae: equilibrium and kinetic modelling. *Proc Biochemist* 40(8):2865–2872
- Mazloomi S, Ghodsei S, Amraei P, Bonyadi Z (2018) Data on the removal of turbidity from aqueous solutions using polyaluminum chloride. *Data Brief* 20:371–374
- Mohammed AA, Kareem SL (2019) Adsorption of tetracycline from wastewater by using Pistachio shell coated with ZnO nanoparticles: equilibrium, kinetic and isotherm studies. *Alex Eng J* 58(3):917–928
- Mohebbad B, Bonyadi Z, Dehghan AA, Rahmat MH (2019) Arsenic removal from aqueous solutions using *Saccharomyces cerevisiae*: kinetic and equilibrium study. *Env Prog* 38(s1):S398–S402
- Nasoudari E, Ameri M, Shams M, Ghavami V, Bonyadi Z (2021) The biosorption of Alizarin Red S by *Spirulina platensis*; process modelling, optimisation, kinetic and isotherm studies. *Int J Environ Anal Chem* 87:1–15
- Neha G, Kushwaha AK, Chattopadhyaya M (2011) Kinetics and thermodynamics of malachite green adsorption on banana pseudostem fibers. *J Chem Pharm Res* 3(1):284–296
- Omar H, El-Gendy A, Al-Ahmary K (2018) Bioremoval of toxic dye by using different marine macroalgae. *Turk J Bot* 42(1):15–27
- Preeti K, Veena S (2017) Bioremediation of textile dyes by using blue green algae. *Int J Sci Res Dev* 5(03):1322–1324
- Ramavandi B, Najafpoor AA, Alidadi H, Bonyadi Z (2019) Alizarin red-S removal from aqueous solutions using *Saccharomyces cerevisiae*: kinetic and equilibrium study. *Desalin Water Treat* 144:286–291
- Rangabhashiyam S, Lata S, Balasubramanian P (2018) Biosorption characteristics of methylene blue and malachite green from

- simulated wastewater onto *Carica papaya* wood biosorbent. *Surf Interf* 10:197–215
- Rezaee A, Ramavandi B, Ganati F (2006a) Equilibrium and spectroscopic studies on biosorption of mercury by algae biomass. *Pakistan J Biolog Sci* 9:777–782
- Rezaee A, Ramavandi B, Ganati F, Ansari M, Solimani A (2006b) Biosorption of mercury by biomass of filamentous algae *Spirogyra* species. *J Biolog Sci* 6:695–700
- Sadeghi A, Ehrampoush MH, Ghaneian MT, Najafpoor AA, Fallahzadeh H, Bonyadi Z (2019) The effect of diazinon on the removal of carmoisine by *Saccharomyces cerevisiae*. *Desalin Water Treat* 137:273–278
- Saha P, Chowdhury S, Gupta S, Kumar I, Kumar R (2010) Assessment on the removal of malachite green using tamarind fruit shell as biosorbent. *Clean: Soil, Air, Water* 38(5–6):437–445
- Santhi T, Manonmani S, Vasanthi V, Chang Y (2016) A new alternative adsorbent for the removal of cationic dyes from aqueous solution. *Arab J Chem* 9:S466–S474
- Signorelli SCM, Costa JM, de Almeida Neto AF (2021) Electrocoagulation-flotation for orange II dye removal: kinetics, costs, and process variables effects. *J Environ Chem Eng* 67:106157
- Sinha AK, Sasmal AK, Pal A, Pal D, Pal T (2021) Ammonium phosphomolybdate [(NH<sub>4</sub>)<sub>3</sub>PMo<sub>12</sub>O<sub>40</sub>] an inorganic ion exchanger for environmental application for purification of dye contaminant wastewater. *J Photochem Photobiol A Chem* 418:113427
- Sun X-F, Wang S-G, Liu X-W, Gong W-X, Bao N, Gao B-Y, Zhang H-Y (2008) Biosorption of Malachite Green from aqueous solutions onto aerobic granules: Kinetic and equilibrium studies. *Bioresour Technol* 99(9):3475–3483
- Tang S, Xia D, Yao Y, Chen T, Sun J, Yin Y, Shen W, Peng Y (2019) Dye adsorption by self-recoverable, adjustable amphiphilic graphene aerogel. *J Colloid Int Sci* 554:682–691
- Veloso CH, Filippov LO, Filippova IV, Ouyard S, Araujo AC (2020) Adsorption of polymers onto iron oxides: Equilibrium isotherms. *J Mater Res Technol* 9(1):779–788
- Wan Y, Liu X, Liu P, Zhao L, Zou W (2018) Optimization adsorption of norfloxacin onto polydopamine microspheres from aqueous solution: Kinetic, equilibrium and adsorption mechanism studies. *Sci Total Environ* 639:428–437

**Publisher's Note** Springer Nature remains neutral with regard to jurisdictional claims in published maps and institutional affiliations.